# CRISPR Repair Reveals Causative Mutation in a Preclinical Model of Retinitis Pigmentosa

Wen-Hsuan Wu[1,2,3], Yi-Ting Tsai[1,2,3], Sally Justus[1,2,3], Ting-Ting Lee[1,2,3], Lijuan Zhang[1,2,3,4], Chyuan-Sheng Lin[5], Alexander G Bassuk[6], Vinit B Mahajan[7,8] and Stephen H Tsang[1,2,3]

*[1]Barbara and Donald Jonas Stem Cell and Regenerative Medicine Laboratory and Bernard and Shirlee Brown Glaucoma Laboratory, Department of Ophthalmology, Institute of Human Nutrition, Herbert Irving Comprehensive Cancer Center, Columbia University, New York, New York, USA; [2]Barbara and Donald Jonas Stem Cell and Regenerative Medicine Laboratory and Bernard and Shirlee Brown Glaucoma Laboratory, Department of Pathology and Cell Biology, Institute of Human Nutrition, Herbert Irving Comprehensive Cancer Center, Columbia University, New York, New York, USA; [3]Edward S. Harkness Eye Institute, New York-Presbyterian Hospital, New York, New York, USA; [4]Shanxi Eye Hospital, Shanxi Medical University, Taiyuan, Shanxi, China; [5]Department of Pathology & Cell Biology, Columbia University Medical Center, New York, New York, USA; [6]Department of Pediatrics and Neurology, University of Iowa, Iowa City, Iowa, USA; [7]Omics Laboratory, University of Iowa, Iowa City, Iowa, USA; [8]Department of Ophthalmology and Visual Sciences, University of Iowa, Iowa City, Iowa, USA*

Massive parallel sequencing enables identification of numerous genetic variants in mutant organisms, but determining pathogenicity of any one mutation can be daunting. The most commonly studied preclinical model of retinitis pigmentosa called the "rodless" (*rd1*) mouse is homozygous for two mutations: a nonsense point mutation (Y347X) and an intronic insertion of a leukemia virus (*Xmv-28*). Distinguishing which mutation causes retinal degeneration is still under debate nearly a century after the discovery of this model organism. Here, we performed gene editing using the CRISPR/Cas9 system and demonstrated that the Y347X mutation is the causative variant of disease. Genome editing in the first generation produced animals that were mosaic for the corrected allele but still showed neurofunction preservation despite low repair frequencies. Furthermore, second-generation CRISPR-repaired mice showed an even more robust rescue and amelioration of the disease. This predicts excellent outcomes for gene editing in diseased human tissue, as *Pde6b*, the mutated gene in *rd1* mice, has an orthologous intron–exon relationship comparable with the human *PDE6B* gene. Not only do these findings resolve the debate surrounding the source of neurodegeneration in the *rd1* model, but they also provide the first example of homology-directed recombination–mediated gene correction in the visual system.

*Received 13 April 2016; accepted 7 May 2016; advance online publication 28 June 2016. doi:10.1038/mt.2016.107*

## INTRODUCTION

A major goal of precision medicine is gene-specific intervention that corrects illness at the nucleotide level, a goal the CRISPR/Cas9 system now puts within reach. Many potential target disease mutations have been implicated by massive parallel sequencing techniques and the Human Genome Project, but the inherent genomic variance between individuals and patterns of polygenic inheritance makes it challenging to distinguish benign variants from pathogenic mutations. Similarly, for mouse models, every inbred line carries its own set of mutations that cumulatively result in its unique characteristics, complicating interpretation of data. A longstanding example of this challenge is found in the $Pde6b^{rd1}/Pde6b^{rd1}$ or "rodless" (*rd1*) mouse,[1] the most extensively studied mouse model of retinitis pigmentosa (RP).

Discovered in 1924, the rd1 mouse has spurred controversy, as the cause of the blinding RP phenotype has been aggressively sought yet remains undetermined. In a "wild-type" (WT) mouse background (*e.g.*, C3H/He, CBA, and FVB/N, the latter two being the primary strains for generation of transgenic mice worldwide), the *rd1* phenotype is linked to two relatively close yet distinct alterations in the *Pde6b* locus of chromosome 5: a murine leukemia virus (*Xmv*-28) insertion in the reverse orientation (3′ to 5′) in intron 1; and a nonsense mutation (Y347X, C to A) in exon 7 of the Pde6β subunit.[2–4] Pde6β functions as part of a heterotetramer, composed of α-, β, and γ-subunits ($\alpha\beta\gamma_2$), that normally downregulates cGMP levels.[5,6] The nonsense mutation in *rd1* mice is thought to truncate more than half of the predicted protein, including the catalytic domain. The consequence is improper regulation of cGMP levels and toxically high $Ca^{2+}$ influx through cyclic nucleotide-gated alpha 1 (CNGA1) cation channels. This is believed to induce rod neuronal death, thus recapitulating the disease course of RP, for which there is no therapeutic cure.

Here, we report the first CRISPR-mediated, homology-directed recombination (HDR) in the retina of a live mouse. Unlike previous ophthalmic gene editing approaches in ablating the diseased allele, we repaired the nonsense point mutation, leaving the *Xmv-28* insertion intact. Our results definitively show that the viral insertion is benign and the Y347X mutation in *rd1* mice to be pathogenic.

## RESULTS

To repair the mutation, we designed a single guide RNA (sgRNA) and a donor template with four wobble-nucleotide

*Correspondence: Stephen H Tsang, Edward S. Harkness Eye Institute, New York-Presbyterian Hospital/Columbia University Medical Center, 635 West 165th Street, Box 112, New York, NY 10032, USA. E-mail: sht2@columbia.edu or Vinit B Mahajan, University of Iowa Hospitals and Clinics, 200 Hawkins Drive, Iowa City, IA, 52242. E-mail: mahajanlab@gmail.com.*

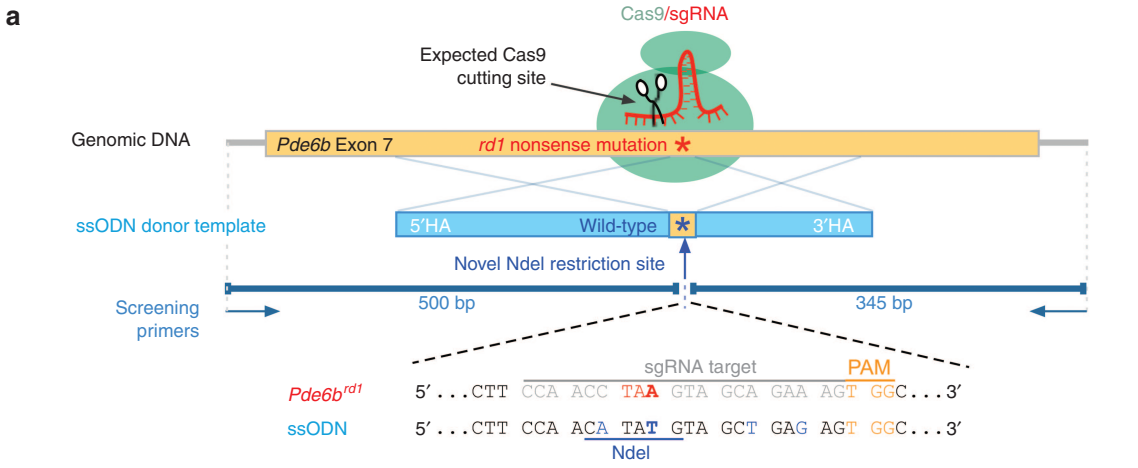


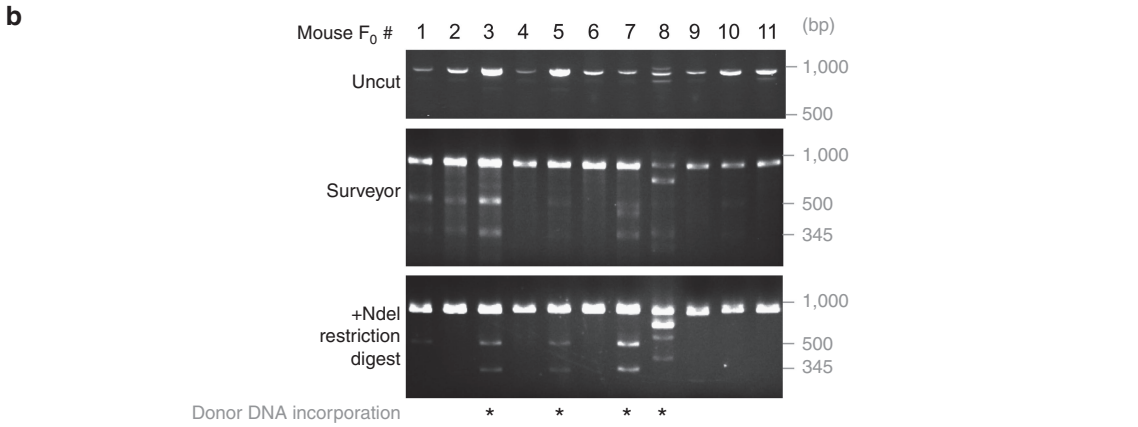


c

| Mouse | Sequence | % Total |
|---|---|---|
| | Y347X PAM | |
| $F_0$3 | Original TGGCCAGTGGCCTTCCAACCTAAGTAGCAGAAAGTGGCTTTGTGAGTGTCCCTCTCCA | 14.2 |
| | HDR TGGCCAGTGGCCTTCCAACATATGTAGCTGAGAGTGGCTTTGTGAGTGTCCCTCTCCA | 35.7 |
| | 1 bp del TGGCCAGTGGCCTTCCAACCTAAGTAGCAGAA-GTGGCTTTGTGAGTGTCCCTCTCCA | 21.4 |
| | 10 bp del TGGCCAGTGGCCTTCCAACCTAAGT----------GGCTTTGTGAGTGTCCCTCTCCA | 28.6 |
| $F_0$5 | Original TGGCCAGTGGCCTTCCAACCTAAGTAGCAGAAAGTGGCTTTGTGAGTGTCCCTCTCCA | 81.2 |
| | HDR TGGCCAGTGGCCTTCCAACATATGTAGCTGAGAGTGGCTTTGTGAGTGTCCCTCTCCA | 18.8 |
| $F_0$7 | Original TGGCCAGTGGCCTTCCAACCTAAGT----------AGCAGAAAGTGGCTTTGTGAG | 43.8 |
| | NHEJ/HDR TGGCCAGTGGCCTTCCAACCTAAGTTCCAACATATGTAGCTGAGAGTGGCTTTGTGAG | 12.5 |
| | 1 bp del TGGCCAGTGGCCTTCCAACCTAAGT----------AGCAGA-AGTGGCTTTGTGAG | 43.8 |
| $F_0$8 | Original TGGCCAGTGGCCTTCCAACCTAAGTAGCAGAAAGTGGCTTTGTGAGTGTCCCTCTCCA | 68.8 |
| | NHEJ 225 bp deletion & 63 insertion | 25.0 |
| | NHEJ 145 bp donor DNA insertion | 6.3 |

**Figure 1 CRISPR/Cas9-mediated repair of Y347X was achieved in a mosaic fashion in 2 of 11 Founders ($F_0$).** (**a**) sgRNA targets *exon 7* of the *Pde6b* locus (yellow box, top). Donor template (blue box, middle) encoding the wild-type allele corrects Y347X through homology-directed recombination. Donor template was made resistant to Cas9 by two modifications: (i) NdeI site and (ii) four wobble base pairs. Primers amplify an 845-bp fragment. (**b**) Surveyor assay reveals that 7 of 11 $F_0$ mice have CRISPR-induced DSBs. NdeI digestion detects correction of Y347X in $F_0$3 and $F_0$5. In $F_0$8 and $F_0$7, INDELs were incorporated alongside the ssODN. (**c**) *Pde6b* was repaired in 35.7% of $F_0$3 and 18.8% of $F_0$5 somatic cells. Allelic heterogeneity due to nonhomologous end joining was apparent as small deletions (1–10 bp) in $F_0$3 and $F_0$7, and large INDELs in $F_0$8, were detected. (Red letters: Y347X mutation; blue letters: wobble nucleotides carried by donor template; yellow letters: PAM sequence; brown letters: INDELs).

substitutions and a novel NdeI restriction site (**Figure 1a**). The substitutions ensured the WT donor template was resistant to targeting, and the NdeI restriction site allowed tracking of HDR. To ensure efficient binding to the target site, four sgRNAs were designed and their targeting efficiency was assessed (**Supplementary Figure S1**); the one with highest binding efficiency was selected. The sgRNA plasmid was coinjected with the single-stranded oligodeoxynucleotide (ssODN) donor template and the Cas9 protein into FVB/N zygotes to generate 11 $F_0$ founders. Tail DNA was analyzed by two methods: Surveyor mismatch-specific endonuclease cleavage assay detected nonhomologous end joining, and a restriction

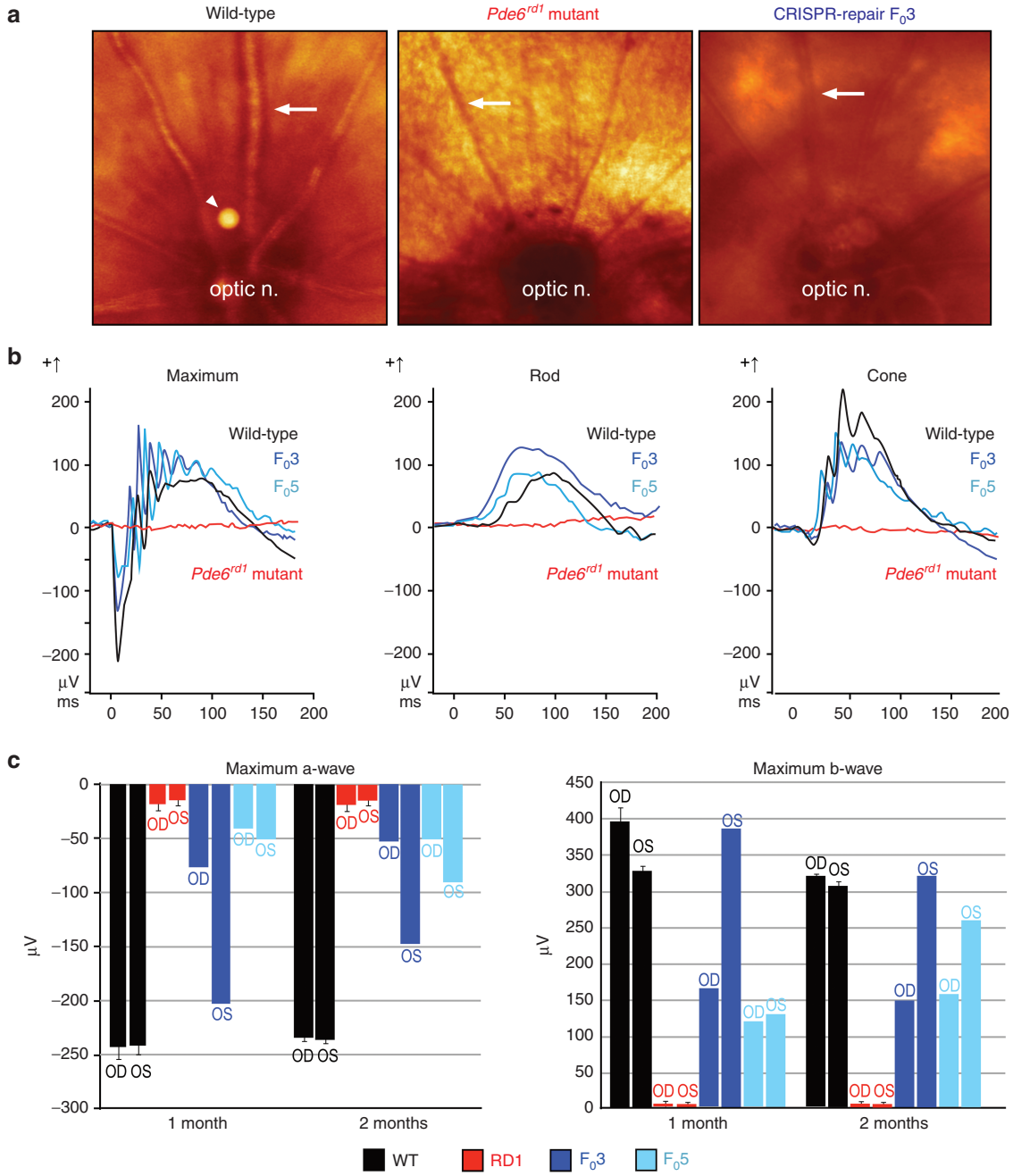


**Figure 2 CRISPR-mediated repair of Y347X in *Pde6b* restored neurophysiology.** (**a**) Uniform coloration of the fundus of an age-matched wild-type (WT) control. "Salt and pepper" retinopathy in the dorsal fundus of the *rd1* mutant as well as vascular attenuation were observed (ON, optic nerve; arrows point to vessels; arrow head points out an imaging artifact). CRISPR-corrected $F_0$3 displays a fundus similar to that of WT, with preservation of vasculature. (**b**) Electroretinogram (ERG) (μV) revealed neurophysiological rescue in 1-month-old gene-corrected mice. *Rd1* mice (red) had extinguished mixed maximum rod–cone, rod-specific, and cone ERG responses. In CRISPR-repaired $F_0$3 (dark blue) and $F_0$5 (light blue) mice, maximum, rod, and cone ERG responses were comparable with WT (black) and significantly heightened compared with the *rd1* mutant. (**c**) Greater magnitude represents improved neurophysiology. Maximum a- and b-wave values obtained at 1 and 2 months in *rd1* (red), $F_0$3 (dark blue), $F_0$5 (light blue), and WT (black) mice. *Rd1* consistently displayed significantly diminished a-waves, which are photoreceptor mediated, and b-waves, which are inner retina mediated. $F_0$3 OS originally registered as nearly equivalent to the WT, but gradually decreased over time. a- and b-wave magnitudes in $F_0$3 OD and $F_0$5 OS/OD were poorer than that of WT but still greater than that of the *rd1* mutant.

fragment polymorphism (RFLP) assay detected HDR events that incorporated the novel NdeI site.

Double-strand breaks were detected in 7 of 11 mice ($F_0$1, 2, 3, 5, 7, 8, 10), indicating that the targeting efficiency of the sgRNA was ~64% (**Figure 1b**). RFLP verified HDR in four animals ($F_0$3, 5, 7, 8), although the molecular weights of the PCR products from $F_0$8 suggested indels were incorporated into the genome alongside the donor template. The target region was sequenced, revealing that $F_0$3 and 5 incorporated the donor template precisely in 35.7% and 18.8% of somatic cells, respectively (**Figure 1c**), while $F_0$7 and

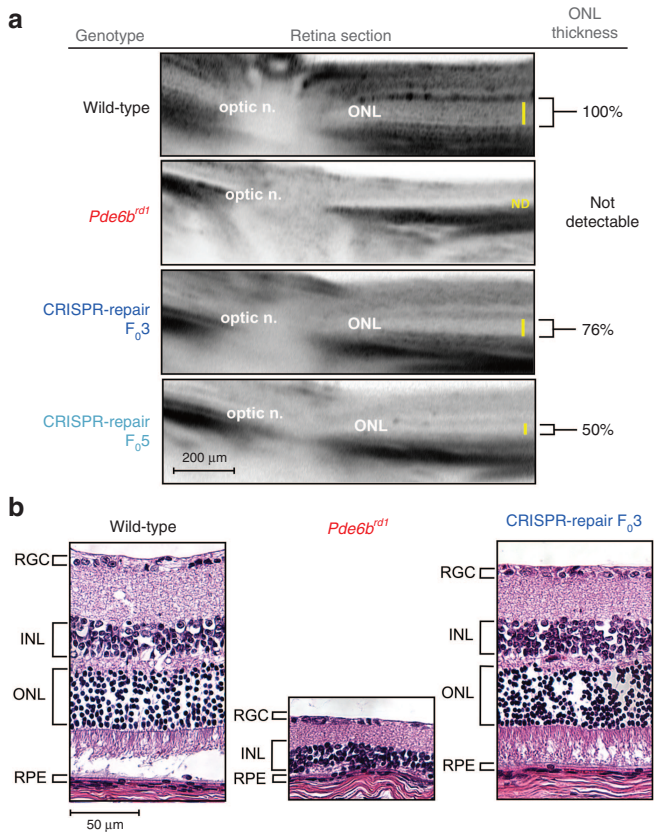


**Figure 3 CRISPR-mediated repair of Y347X in *Pde6b*$^{rd1}$ restored retinal structure.** (**a**) Optical coherence tomography data at 3 months from wild-type (WT), *rd1*, $F_0$3, and $F_0$5 mice reflected partial preservation of retinal layers in the CRISPR-rescued mice compared with the *rd1* mutant. The outer nuclear layer (ONL) was not detectable in *rd1*. Yellow bar indicates the ONL thickness, which was normalized to WT and measured to be 76% and 50% in $F_0$3 and $F_0$5, respectively. (**b**) Hematoxylin–eosin-stained retinal section from WT, *rd1*, and $F_0$3 mice at 3 months revealed that retinal layers were preserved in $F_0$3 and were comparable with that of WT, whereas the *rd1* mutant layers had collapsed and loss the photoreceptor (ONL) layer. INL, inner nuclear layer; RGC, retinal ganglion cell; RPE, retinal-pigmented epithelium.

8 incorporated indels in the integration, corroborating the unexpected results in the RFLP data. These data also reveal that the $F_0$ animals were mosaic, a phenomenon that has been reported previously[7,8] and likely arises from CRISPR/Cas9 repair occurring after the zygote stage.

Live retinal imaging compared CRISPR-repaired and untreated controls to assess whether correction of the Y347X mutation could restore retinal structure (**Figure 2a**). Whereas the *rd1* fundus appeared granulated and its vasculature attenuated by retinopathy, the CRISPR-repaired $F_0$3 fundus coloring was uniform, with robust vessels resembling a WT eye. CRISPR repair of neurofunction was assessed by electroretinogram (ERG) in $F_0$3 and 5, *rd1* mutant, and WT mice (**Figure 2b**). At P30, ERG of Y347X-repaired $F_0$ mice showed that their rod, cone, and mixed rod–cone (maximum) responses were comparable with WT. In contrast, *rd1* no longer displayed an ERG response (**Figure 2b**). This result indicates that neurofunction was restored in Y347X-repaired mice, while light-induced neural responses were lost in the unedited *rd1*. Serially re-recorded ERGs revealed a long-term functional rescue in both $F_0$3 and 5, lasting at least 2 months (**Figure 2c**). Interestingly, in $F_0$3, the right (OD) verses left (OS) eyes differed in their maximum a-wave amplitude (the electrical response of photoreceptors) and b-wave amplitude (the response of optic nerve-bipolar cells). Dissimilarities in ERG responses between eyes from the same mouse suggest that the CRISPR-mediated correction was mosaic. This outcome aligns with other studies that demonstrated a greater degree of rescue in tissues containing a higher prevalence of CRISPR-mediated repair.[9] While $F_0$3 and 5 both had robust ERG rescues compared with *rd1*, their a- and b-wave magnitudes were not completely restored to that of WT, which can be explained by the low HDR rate. Notably, $F_0$3, with 35.7% of somatic cells corrected, had amplitudes closer to WT levels than did $F_0$5, with only 18.8% of cells corrected, verifying the dose-dependent rescue observed in other studies.[9] This confirms that correcting every cell is not necessary for preservation of ERG function or to halt degeneration,[10,11] as a 35.7% HDR in photoreceptors was sufficient for restoration of ERG wave amplitudes (**Figure 2c**).

In $F_0$ founder, these functional data were corroborated by optical coherence tomography (OCT) live imaging, which indicated that a partial rescue of the outer nuclear layer, which contains photoreceptor nuclei, was achieved in $F_0$3 and 5 (76% and 50% of normal thickness, respectively) as far out as P90 (**Figure 3a**). In histopathological studies, CRISPR-repaired $F_0$ had normal retinal layers, with photoreceptor nuclei density comparable with WT, whereas the retinal layers of *rd1* had collapsed (**Figure 3b**). These data, combined with ERG functional analysis, indicate that greater rescue cause greater retinal preservation, as $F_0$3 (35.7% correction) showed greater a- and b-wave magnitudes and thicker retinal sections on OCT compared with $F_0$5 (18.8% correction).

To assess whether the mosaic pattern of expression in the eyes was also prevalent throughout the body, organs were collected and subjected to RFLP assay. In $F_0$3 and 5, cells containing the repaired or uncorrected alleles were uniformly distributed among organs regardless of the organ's developmental origin, with 32–37% of somatic cells corrected in $F_0$3 and 11–20% corrected in $F_0$5 (**Figure 4a**). This implies that CRISPR/Cas9-mediated repair occurred after the zygote stage but before the preimplantation stage. Additionally, the correction levels were the highest in the retina in both mice. This is because by P90, the cells that did not contain the correction likely died, increasing the ratio of corrected cells.

Backcrossing $F_0$3 with homozygous *rd1* mice produced 10 $F_1$ mice, three of which ($F_1$1, 2, and 3) contained the ssODN-corrected allele (**Figure 4b**). ERG functional assay of $F_1$1 displayed results comparable with WT (**Figure 4c**). OCT comparing wild-type and $F_1$1 showed robust rescue of the outer nuclear layer (90% the thickness of WT) (**Figure 4d**). These data show that the correction in $F_0$ is mosaic in the germ line, and it is passed on in a non-Mendelian fashion to the $F_1$ generation, which have a near complete functional and morphological rescue.

The *Pde6b*$^{rd1}$ locus also harbors an *Xmv-28* provirus integrated into the first intron (**Figure 4e**), which has been suspected to be the cause of pathogenesis[2,3] in the *rd1* preclinical model. This possibility seems less likely, since PCR analysis of $F_0$3 and 5, and $F_1$1, 2, and 3 confirmed the presence of the *Xmv-28* insertion, even after

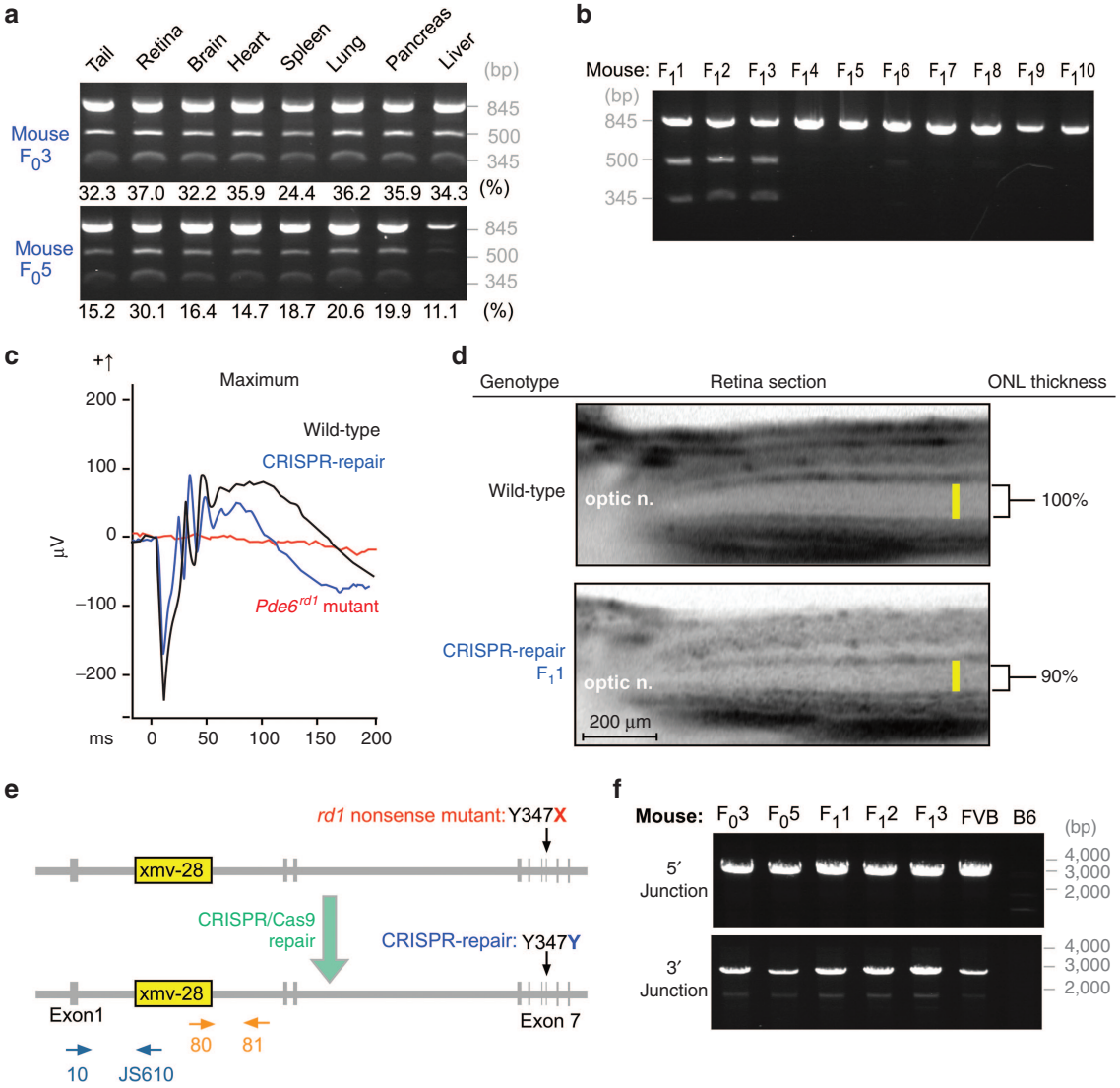


**Figure 4** *Xmv-28* **viral insertion was retained but benign in gene-repaired mice.** (**a**) Restriction fragment polymorphism (RFLP) revealed CRISPR-mediated correction in 24–37% of cells comprising organs in $F_0$3, and 11–30% in $F_0$5. Data show that the CRISPR-mediated correction occurred at preimplantation, since repaired and uncorrected alleles were uniformly distributed in endoderm, mesoderm, and ectoderm organ lineages. (**b**) RFLP demonstrates that $F_0$3 backcrossed with the *Rd1* mutant transmitted the corrected Y347X allele to 3 of 10 offspring ($F_1$1, 2, and 3). (**c**) Mixed maximal rod–cone electroretinogram (ERG) recordings from $F_1$ at P30. $F_1$1 (blue) registered a- and b-wave amplitudes similar to that of the wild-type (WT) control (black); *rd1* (red) registered a flat ERG. (**d**) Optical coherence tomography compared retinal layer thicknesses in WT and $F_1$1. The latter's outer nuclear layer (ONL) was 90% of WT thickness, confirming rescue was transmitted to $F_1$. (**e**) Schematic representation of the *Xmv-28* insertion (yellow box). CRISPR repairs the Y347X mutation (red), restoring it to the WT sequence (blue) while leaving the insertion intact. Dark blue and orange arrows represent primers used to screen the 5′ and 3′ ends of the viral insertion. Primer 10 targeted *Pde6b* exon 1, while JS610 targeted the *Xmv-28 env* gene, together amplifying the 5′ end of the insertion. Primer 81 targeted intron 1 of *Pde6b*, while primer 80 targeted the *Xmv-28 gag* gene, together amplifying the 3′ end of the insertion. (**f**) PCR confirmed that *Xmv*-28 insertion was retained in CRISPR/Cas9-repaired *rd1* mice. This suggests that the Y347X mutation, rather than the viral insertion, causes the disease phenotype.

CRSIPR-mediated restoration of the WT phenotype (**Figure 4f**). Complete restoration of neuronal function and structure by correction of the Y347X mutation suggests that the *Xmv-28* provirus insertion is clinically irrelevant to the disease phenotype in *rd1* mice. Hence, our data resolve this controversy by demonstrating that repair of the nonsense mutation is sufficient to restore the WT phenotype, even while leaving the *Xmv-28* insertion intact in the genome.

## DISCUSSION

Mutations in the human *rd1* gene, *PDE6B*, are responsible for 36,000 cases of RP worldwide each year,[6,12–14] and the ability for CRISPR-mediated gene therapy to rescue photoreceptors in preclinical models is encouraging for both researchers and patients alike. The improvement in mosaic animals was also seen in a gene correction of Duchenne muscular dystrophy)[9] and suggests that postnatal CRISPR delivery systems might eventually be developed into a precision medicine protocol that can safely restore retinal function in adults.[8] Indeed, we previously showed both adeno-associated virus (AAV) and lentivirus-mediated gene therapy approaches could efficiently deliver functional genes to retinal cells, and we observed marked efficacy even in photoreceptor mosaics.[10,11,15–18] Results from **Figure 2** suggest that

CRISPR repair of the diseased allele in only a fraction of the cells can have significant therapeutic effects.

More importantly, our results extend beyond identifying the causative mutation in the strains most frequently studied in transgenesis. This CRISPR clarification approach is applicable to any condition where two or more single-nucleotide polymorphisms associated with disease pathology have yet to be distinguished, including inflammatory bowel diseases, schizophrenia, autism, Parkinson's, and age-related macular degeneration,[19] among others. To determine which variant should in fact be targeted, each could be swapped via CRISPR-mediated HDR, creating isogenic lines that differ by a single allele. In this way, suspected mutations could be systematically screened and characterized. As the efficacy of CRISPR is enhanced and the off-targeting effects are reduced, the translational utility of this technique will only continue to increase.

## MATERIALS AND METHODS

***Mouse lines and husbandry.*** FVB/N mice, which are inbred and homozygous for the retinal degeneration 1 allele of *Pde6b*$^{rd1}$, were purchased from The Jackson Laboratory, (Bar Harbor, ME). Albino B6 (Cg)-*Tyr*$^{C-2J}$/J mice were used as the normal control and FVB/N mice without CRISPR-mediated correction as the functional-deficient control. All mice were used in accordance with the Statement for the Use of Animals in Ophthalmic and Vision Research of the Association for Research in Vision and Ophthalmology, as well as the Policy for the Use of Animals in Neuroscience Research established by the Society for Neuroscience.

***sgRNA construction.*** pX335 was obtained from Addgene.[20] Complimentary oligonucleotides (Integrated DNA Technologies, Iowa, IA) containing the *Pde6b* sgRNA target sequences (**Figure 1**) were annealed and cloned into the BbsI site of pX335. This plasmid (RD1-sgRNA_pX335) was then sequenced to verify correct insertion of the target sequences.

***RNA injections into mouse zygotes.*** A mixture of 3 ng/μl of sgRNA plasmid, 3 ng/μL of Cas9 protein (NEB, Ipswich, MA), and 1 μM of ssODN (Integrated DNA Technologies) was injected into the pronuclei and cytoplasm of FVB/N inbred zygotes. Zygotes that survived injection were transferred into oviducts of 0.5-day postcoitum, pseudopregnant B6xCBA F1 females and carried to term. The resulting gene-corrected mice were backcrossed, initially into the FVB/N background, to determine the germline transmission efficiency of the repair.

***Detection of gene correction and nonhomologous end joining.*** To identify CRISPR/Cas9-mediated gene correction in the *Pde6b*$^{rd1}$ locus, tail genomic DNA from mice with zygote injections was isolated and amplified by PCR, using the primer set: RD1-check-F: 5′-caagaaggcagtaggattccg-3′ and RD1-check-R: 5′-ttgtcttgcctgcttctcatc-3′. The amplified products were subjected to NdeI restriction enzyme digestion. For detecting nonhomologous end joining, PCR products were analyzed by the Surveyor assay (Integrated DNA Technologies, Iowa, IA). PCR products of mouse F0, 5, 7, and 8 were subcloned into pCR™4Blunt-TOPO® vector (Invitrogen, Carlsbad, CA). Individual clones were sequenced and compared with WT. Sixteen clones were sequenced from each mouse. To detect mosaicism, 3-month-old $F_0$ mice were sacrificed, and genomic DNA from organs was harvested and subjected to PCR following the RFLP assay.

***Analysis of Xmv-28 insertion.*** PCR analysis of Xmv-28 insertion was performed according to Bowes *et al.*[3] Briefly, a 3.3-kb DNA sequence of the 5′ junction was amplified using primers 10: 5′- ATGTA CCGCCAGCGCAATGG-3′ and JS610: 5′- CCCCGCCTTCTCAACAACC TGGGACGGGAG-3′, which recognizes the sequence of exon 1 of the *Pde6b*$^{rd1}$ gene and the env gene of Xmv-28, respectively. A 2.4-kb DNA sequence of 3′ junction that spans the 5′ LTR of Xmv-28 and flanking genomic *Pde6b*$^{rd1}$ sequences was amplified using primers 80: 5′- CTCTGTTTCTCTCCTGATACG-3′ and 81: 5′- ACCT GCATGTGAACCCAGTATT-3′.

***Electroretinograms.*** Electroretinograms (ERGs) were conducted as described.[11,17] In dark-adapted mice, rod and mixed rod–cone responses were obtained using pulses of 0.001 and 3 cd × s/m$^2$ (white 6,500 K) light, respectively, while cone responses were recorded under rod-suppressing continuous background illumination of 30 cd/m$^2$ (white 6,500 K) using pulses of 30 cd × s/m$^2$ (xenon). ERG a- and b-wave magnitudes and maximal scotopic and photopic recordings were collected serially at 1 and 2 months in $F_0$ and $F_1$.

***Fundoscopy and autofluorescence imaging.*** Infrared images were obtained with the Spectralis scanning laser confocal ophthalmoscope (OCT-SLO Spectralis 2; Heidelberg Engineering, Heidelberg, Germany) as previously described.[10,11,17,18,21,22] Autofluorescence imaging was performed as described previously.[10,11,17,18,21,22]

***Histology.*** H&E histology was carried out as previously described.[23,24]

***Statistics.*** Data were collected in Excel, and statistical analyses used the two-tailed unpaired *t*-test and error bars display the mean value ± standard deviations. $P < 0.05$ was considered to be statistically significant.

## SUPPLEMENTARY MATERIAL

**Figure S1.** *In vitro* digestion assay demonstrates targeting efficiency of sgRNA.

## REFERENCES


1. Pittler, SJ, Keeler, CE, Sidman, RL and Baehr, W (1993). PCR analysis of DNA from 70-year-old sections of rodless retina demonstrates identity with the mouse rd defect. *Proc Natl Acad Sci USA* **90**: 9616–9619.
2. Bowes, C, Li, T, Danciger, M, Baxter, LC, Applebury, ML and Farber, DB (1990). Retinal degeneration in the rd mouse is caused by a defect in the beta subunit of rod cGMP-phosphodiesterase. *Nature* **347**: 677–680.
3. Bowes, C, Li, T, Frankel, WN, Danciger, M, Coffin, JM, Applebury, ML *et al.* (1993). Localization of a retroviral element within the rd gene coding for the beta subunit of cGMP phosphodiesterase. *Proc Natl Acad Sci USA* **90**: 2955–2959.
4. Pittler, SJ and Baehr, W (1991). Identification of a nonsense mutation in the rod photoreceptor cGMP phosphodiesterase beta-subunit gene of the rd mouse. *Proc Natl Acad Sci USA* **88**: 8322–8326.
5. Keeler, CE (1928). The geotropic reaction of rodless mice in light and in darkness. *J Gen Physiol* **11**: 361–368.
6. McLaughlin, ME, Ehrhart, TL, Berson, EL and Dryja, TP (1995). Mutation spectrum of the gene encoding the beta subunit of rod phosphodiesterase among patients with autosomal recessive retinitis pigmentosa. *Proc Natl Acad Sci USA* **92**: 3249–3253.
7. Yang, H, Wang, H, Shivalila, CS, Cheng, AW, Shi, L and Jaenisch, R (2013). One-step generation of mice carrying reporter and conditional alleles by CRISPR/Cas-mediated genome engineering. *Cell* **154**: 1370–1379.
8. Long, C, Amoasii, L, Mireault, AA, McAnally, JR, Li, H, Sanchez-Ortiz, E *et al.* (2016). Postnatal genome editing partially restores dystrophin expression in a mouse model of muscular dystrophy. *Science* **351**: 400–403.
9. Long, C, McAnally, JR, Shelton, JM, Mireault, AA, Bassel-Duby, R and Olson, EN (2014). Prevention of muscular dystrophy in mice by CRISPR/Cas9-mediated editing of germline DNA. *Science* **345**: 1184–1188.
10. Davis, RJ, Hsu, CW, Tsai, YT, Wert, KJ, Sancho-Pelluz, J, Lin, CS *et al.* (2013). Therapeutic margins in a novel preclinical model of retinitis pigmentosa. *J Neurosci* **33**: 13475–13483.
11. Koch, SF, Tsai, YT, Duong, JK, Wu, WH, Hsu, CW, Wu, WP *et al.* (2015). Halting progressive neurodegeneration in advanced retinitis pigmentosa. *J Clin Invest* **125**: 3704–3713.
12. Bird, AC (1995). Retinal photoreceptor dystrophies LI. Edward Jackson Memorial Lecture. *Am J Ophthalmol* **119**: 543–562.
13. Hartong, DT, Berson, EL and Dryja, TP (2006). Retinitis pigmentosa. *Lancet* **368**: 1795–1809.
14. Daiger, SP, Bowne, SJ and Sullivan, LS (2007). Perspective on genes and mutations causing retinitis pigmentosa. *Arch Ophthalmol* **125**: 151–158.
15. Davis, RJ, Tosi, J, Janisch, KM, Kasanuki, JM, Wang, NK, Kong, J *et al.* (2008). Functional rescue of degenerating photoreceptors in mice homozygous for a hypomorphic cGMP phosphodiesterase 6 b allele (Pde6bH620Q). *Invest Ophthalmol Vis Sci* **49**: 5067–5076.
16. Tosi, J, Davis, RJ, Wang, NK, Naumann, M, Lin, CS and Tsang, SH (2011). shRNA knockdown of guanylate cyclase 2e or cyclic nucleotide gated channel alpha 1 increases photoreceptor survival in a cGMP phosphodiesterase mouse model of retinitis pigmentosa. *J Cell Mol Med* **15**: 1778–1787.

17. Wert, KJ, Skeie, JM, Bassuk, AG, Olivier, AK, Tsang, SH and Mahajan, VB (2014). Functional validation of a human CAPN5 exome variant by lentiviral transduction into mouse retina. *Hum Mol Genet* **23**: 2665–2677.
18. Wert, KJ, Sancho-Pelluz, J and Tsang, SH (2014). Mid-stage intervention achieves similar efficacy as conventional early-stage treatment using gene therapy in a pre-clinical model of retinitis pigmentosa. *Hum Mol Genet* **23**: 514–523.
19. Yang, J, Li, Y, Chan, L, Tsai, YT, Wu, WH, Nguyen, HV *et al.* (2014). Validation of genome-wide association study (GWAS)-identified disease risk alleles with patient-specific stem cell lines. *Hum Mol Genet* **23**: 3445–3455.
20. Cong, L, Ran, FA, Cox, D, Lin, S, Barretto, R, Habib, N *et al.* (2013). Multiplex genome engineering using CRISPR/Cas systems. *Science* **339**: 819–823.
21. Tsang, SH, Gouras, P, Yamashita, CK, Kjeldbye, H, Fisher, J, Farber, DB *et al.* (1996). Retinal degeneration in mice lacking the gamma subunit of the rod cGMP phosphodiesterase. *Science* **272**: 1026–1029.
22. Tsang, SH, Burns, ME, Calvert, PD, Gouras, P, Baylor, DA, Goff, SP *et al.* (1998). Role for the target enzyme in deactivation of photoreceptor G protein in vivo. *Science* **282**: 117–121.
23. Mahajan, VB, Skeie, JM, Assefnia, AH, Mahajan, M and Tsang, SH (2011). Mouse eye enucleation for remote high-throughput phenotyping. *J Vis Exp* **57**: 3184.
24. White, JK, Gerdin, AK, Karp, NA, Ryder, E, Buljan, M, Bussell, JN *et al.*; Sanger Institute Mouse Genetics Project. (2013). Genome-wide generation and systematic phenotyping of knockout mice reveals new roles for many genes. *Cell* **154**: 452–464.